Journal of Energetic Materials
Publication details, including instructions for authors and subscription information:
http://www.informaworld.com/smpp/title~content=t713770432

Kinetics and mechanism of the thermal decomposition of dimethylnitramine at low temperatures

S. A. Lloyd[a]; M. E. Umstead[a]; M. C. Lin[a]
[a] Chemistry Division Code 6105, Naval Research Laboratory, Washington, D.C.

To cite this Article Lloyd, S. A. , Umstead, M. E. and Lin, M. C.(1985) 'Kinetics and mechanism of the thermal decomposition of dimethylnitramine at low temperatures', Journal of Energetic Materials, 3: 3, 187 — 210
To link to this Article: DOI: 10.1080/07370658508010624
URL: http://dx.doi.org/10.1080/07370658508010624

KINETICS AND MECHANISM OF THE THERMAL DECOMPOSITION OF DIMETHYLNITRAMINE AT LOW TEMPERATURES

S. A. Lloyd,* M. E. Umstead, and M. C. Lin

Chemistry Division
Code 6105
Naval Research Laboratory
Washington, D.C. 20375-5000

ABSTRACT

Dimethylnitramine (DMNA) was pyrolyzed between 466 and 524 K at about 475 Torr pure DMNA pressure in static cells. A radical mechanism was proposed and computer-modeled to account for the disappearance of DMNA and the production of $(CH_3)_2NNO$ and CH_3NO_2. The rate constant for DMNA decomposition into $(CH_3)_2N$ and NO_2, based on these low-temperature results and other high-temperature shock tube data, covering 460-960 K, can be given by $k_1 = 10^{15.9\pm0.2} \exp(-22{,}000\pm200/T)$ sec^{-1}. This result leads to values for the N-N bond energy of 43.3±0.5 kcal/mole and the heat of formation of the $(CH_3)_2N$ radical, 35±2 kcal/mole at 298 K. Kinetic modeling of the CH_3NO_2 and $(CH_3)_2NNO$ production profiles has been carried out.

---

*Federal Junior Fellow, 1980-1985

Journal of Energetic Materials vol. 3, 187-210 (1985)

Published in 1985 by Dowden, Brodman & Devine, Inc.

INTRODUCTION

Dimethylnitramine (DMNA) is the simplest stable nitramine molecule. Although the decomposition of DMNA has been studied previously, the sketchy mechanism proposed by Flournoy[1] in 1962 and adopted by later researchers does not account for the production of any stable products other than dimethylnitrosamine (DMNSA):

$$(CH_3)_2NNO_2 \longrightarrow (CH_3)_2N + NO_2 \quad (1)$$

$$(CH_3)_2NNO_2 + NO_2 \longrightarrow NO + \text{oxidation products} \quad (2)$$

$$(CH_3)_2N + NO \longrightarrow (CH_3)_2NNO. \quad (3)$$

In the above mechanism, reaction (2) was proposed to qualitatively provide the needed NO molecule for DMNSA formation. DMNSA is the major low-temperature product which accounts for more than 80% of the decomposed DMNA. The validity of reaction (2) is, however, theoretically quite questionable. On the basis of the measured DMNSA yields, Flournoy[1] obtained the rate constant for the unimolecular decomposition of DMNA:

$$k_1 = 10^{20} \exp(-26{,}700/T) \text{ sec}^{-1} \quad (I)$$

The Arrhenius parameters given by Eqn. (I), particularly the A-factor (which is questionable for a gas phase reaction), differ significantly from those reported by Korsunskii et. al[2,3]

$$k_1 = 10^{14.1} \exp(-20{,}500 \pm 900/T) \text{ sec}^{-1} \quad (II)$$

$$k_1 = 10^{13.7} \exp(-19{,}600/T) \text{ sec}^{-1} \quad (III)$$

evaluated from total pressure change measurements. By very low-pressure pyrolysis McMillen et al.[4] obtained the expression

$$k_1 = 10^{16.5\pm0.8} \exp(-24{,}400\pm900/T)\ \text{sec}^{-1} \qquad \text{(IV)}$$

and for a second channel involving HONO elimination:

$$k_{HONO} = 10^{12.4\pm0.8} \exp(-16{,}600\pm900/T)\ \text{sec}^{-1} \qquad \text{(V)}$$

In this work the rate constant for the unimolecular decomposition of DMNA was carefully measured by direct product analysis, and a radical mechanism accounting quantitatively for the production of DMNSA and CH_3NO_2 was proposed and computer modeled.

EXPERIMENTAL

DMNA was prepared by the dehydration of dimethylamine nitrate[5] and recrystallized four times from diethyl ether until no trace of the major by-product, DMNSA, could be detected by gas chromatography. Four Pyrex bulbs (approx. 59 ml) were filled with 70-90 mg crystalline DMNA to yield a pressure of about 475 Torr at the pyrolysis temperature. The bulbs were degassed rapidly (to minimize loss of DMNA) and reweighed. The bulbs were immersed in a stirred, temperature-controlled oil bath (ThermisTemp Model 63 temperature controller, Dow Corning 210H silicon oil) for periods of 15 min. to five hours. After pyrolysis the bulbs were cooled rapidly to room temperature with tap water and then to

195 K in an isopropanol/dry ice slush to freeze out the nonvolatile products. Stable gas products (CH_4, CO and CO_2) were analyzed on a Beckman GC-4 gas chromatograph equipped with a low-pressure gas sampling loop.[6] The gases were separated on 2-meter Porapak-T and Molecular Sieve-5A columns. CO and CO_2, after separation from other components, were reduced on a Ni catalyst to CH_4 for detection by a flame ionization detector. Ethane, ethylene and acetylene were not detected. The bulbs were then warmed to room temperature and the condensed products dissolved in 10 ml H_2O. DMNA, DMNSA and CH_3NO_2 were separated on a 2-meter 5% tris(cyanoethoxy)propane on Gas-Chrom RZ, 60/80 mesh, column at 393 K. Two very small peaks with short retention times were tentatively identified as CH_3OH and CH_3ONO. Methylamine, dimethylamine and trimethylamine were not detected in the liquid samples.

RESULTS

The disappearance of DMNA as a function of time is plotted in Figure 1 for six temperatures between 466 and 525 K. From the slopes of these first-order plots, we obtained the unimolecular rate constants for the initiation reaction,

$$(CH_3)_2NNO_2 \longrightarrow (CH_3)_2N + NO_2 \qquad (1)$$

A least-squares analysis of the values of k_1 for eleven temperatures summarized in Figure 2, taking into account deviations in temperature recorded during the individual experiments, leads to

$$k_1 = 10^{16.45\pm0.45} \exp(-22{,}850\pm550/T) \text{ sec}^{-1} \qquad \text{(VI)}$$

for the temperature range 466-525 K. This result agrees reasonably with Eqn. (IV) obtained by McMillen et al.[4]

It should be noted that the values of k_1 obtained from these low-temperature, high-pressure experiments were found to be independent of pressure. The addition of 881 torr of toluene, for example, did not affect k_1 (see the solid point in Figure 2). This observation also suggests the absence of long-chain reactions at these low temperatures. Toluene has long been used as an effective radical scavenger in pyrolytic systems. This finding was further supported by the results of our kinetic modeling which showed that the presence of CH_3 and CH_3O radicals in this system should have a negligible effect on the unimolecular decay of DMNA. The lines shown in Figure 1 are the kinetically modeled values. A more detailed discussion of kinetic modeling will be made later.

The major early products of DMNA decomposition in this temperature range are DMNSA and CH_3NO_2. The yields of DMNSA are typically about 5-10 times higher that those of CH_3NO_2, depending on the temperature. Figures

3 and 4 show the yields of these two early products, together with the concentrations of DMNA, at 490 and 513 K. The curves shown in these figures are the computed ones.

In addition to these two organic products, smaller amounts of CH_4, CO and CO_2 were also detected, along with trace amounts of other organic products (possibly CH_3OH and CH_3ONO). No attempts were made to interpret their formation because of their low yields. The measured yields of CO and CO_2 (which are much higher than the calculated ones) are believed to be unreliable due to possible low-temperature reactions taking place before the products could be analyzed. At the end of each pyrolysis experiment a red-brown gas, presumably NO_2, was observed in each of the reaction bulbs and was noted to disappear within a few minutes after the bulbs were cooled to room temperature. Both CO and CO_2 could be formed by the reaction of NO_2 with CH_2O or CH_3OH in the liquid phase or heterogeneously on the cell wall.

DISCUSSION

Unimolecular Decomposition of DMNA

The thermal decomposition of DMNA is believed to take place primarily by N-N bond breaking, generating $(CH_3)_2N$ and NO_2:[1-4,7,8]

$$(CH_3)_2NNO_2 \longrightarrow (CH_3)_2N + NO_2 \qquad (1)$$

In a separate study at higher temperatures using a shock tube we have recently measured the initial rates of DMNA decomposition by UV absorption at 254 nm.[9] The results of this study, after appropriate corrections for pressure effects, are in full agreement with the present low-temperature data. Both sets of data are summarized in Figure 5 for comparison. A least-squares fit of these data, covering the 460-960 K temperature range with the magnitude of k_1 values changed by eleven decades, gave rise to the expression,

$$k_1 = 10^{15.9\pm0.2} \exp(-22{,}200\pm200/T) \text{ sec}^{-1}. \qquad \text{(VII)}$$

The absence of curvature in the Arrhenius plot and the reasonableness of the A-factor, in comparison with those given by Eqs. (I)-(III), suggest the absence of other competitive decomposition channels, such as the one leading to HONO formation,[4,10]

$$(CH_3)_2NNO_2 \longrightarrow CH_3NCH_2 + HONO$$

which requires a much smaller A-factor. The results of a recent IRMPD (infrared multiphoton dissociation) experiment, carried out in a molecular beam system, unequivocally support this conclusion.[11]

The activation energy for reaction (1), 44.1±0.4 kcal/mole, after a minor temperature correction to 298 K, gives rise to

$$D(>N\text{-}NO_2) = 43.3 \pm 0.5 \text{ kcal/mole}$$

and

$\Delta H_f°_{,298}$ [$(CH_3)_2N$] = 35±2 kcal/mole,

assuming $\Delta H_f°_{,298}$ (DMNA) =- 0.2±1.2 kcal/mole[12], and the activation energy for the reverse association reaction to be negligible. The heat of formation of $(CH_3)_2N$ given above agrees closely with the recommended value, 34.7±2 kcal/mole.[13]

Kinetic Modeling

The question of the conversion of $(CH_3)_2NNO_2$ into $(CH_3)_2NNO$, the major low temperature pyrolysis product, is mechanistically a very interesting one. Flournoy[1] was correct in not invoking the direct production of DMNSA by N-O split which is energetically too endothermic to be important. Flournoy's assumption of reaction (2), however, is theoretically unsound and practically groundless. Experimentally, we found that mixtures of DMNA and NO_2 are stable over a long period of time at room temperature. Similarily, mixtures of DMNSA and NO_2 after long standing did not appear to have undergone reaction. Accordingly, we propose[7,8] that the production of NO as well as the CH_3 radical, which is required to account for the observed CH_3NO_2 product, occurs via the following exothermic reaction:

$$(CH_3)_2N + NO_2 \longrightarrow (CH_3NO)_2 \longrightarrow 2CH_3NO \qquad (2a)$$

$$\Delta H^\circ_{2a} \simeq -11 \text{ kcal/mole}$$

The energetic diagram as well as the mechanism of this reaction is shown in Figure 6. At low temperatures, the occurrence of this reaction may be aided by the formation of the $(CH_3NO)_2$ dimer, which is stable with respect to CH_3NO by about 23 kcal/mole[14]. The needed NO molecule for DMNSA production via reaction (3):

$$(CH_3)_2N + NO \longrightarrow (CH_3)_2NNO, \qquad (3)$$

can be formed by the unimolecular decomposition of CH_3NO:

$$CH_3NO \longrightarrow CH_3 + NO. \qquad (4)$$

This is expected to be followed by the rapid bimolecular reactions involving CH_3 and NO_2:

$$CH_3 + NO_2 \longrightarrow CH_3NO_2 \qquad (5)$$

$$\longrightarrow CH_3O + NO. \qquad (6)$$

All the decomposition and recombination reactions given above can be shown to take place at their high-pressure limits under the present conditions by means of the RRKM theory.

The value of the rate constant for CH_3NO decomposition was computed by using its reverse rate obtained by Basco et al.[15] The calculated expression by means of the RRKM theory is summarized in Table I, together with other rate constants employed in the present modeling, including the modeled values for k_{2a}, k_3 and k_5. These three rate constants for the radical-radical combination

processes were taken to be independent of temperatures in the range of 466-525 K. The result of an RRKM calculation for k_{2a}, for example, supports this assumption.

The computed DMNSA and CH_3NO_2 production profiles over the whole range of temperature studied agree closely with the observed ones using the values of these three rate constants as given. The results of 490 and 514 K are shown in Figures 3 and 4, respectively. It should be mentioned that the value of k_3 for $(CH_3)_2N$ + NO, 2×10^{11} cc/mole.sec agrees closely with that estimated by Gowenlock and Snelling, $\sim 1 \times 10^{11}$ cc/mole.sec.[16] It is also important and reassuring to note that the values of the k_5 obtained from this modeling, as summarized in Table II, fall within the range of $2.2 \pm 0.5 \times 10^{12}$ cc/mole.sec. This value is in satisfactory agreement with the literature values, $1\text{-}12 \times 10^{12}$ cc/mole.sec (see footnote of Table II). The correctness of the value of k_5 from this modeling supports the reasonableness of the mechanism proposed.

In the low-temperature mechanism summarized in Table I, the decomposition of the CH_3O radical producing CH_2O + H was not included. It was found to be unimportant under the conditions employed. It is, however, a key chain-carrying process at high temperatures in shock-heated DMNA decomposition reactions[9].

The key conclusions reached from the present modeling are summarized as follows:

a. At low temperatures, the disappearance of DMNA occurs primarily via the unimolecular decomposition process (1). Its destruction by bimolecular reactions involving CH_3 and CH_3O are unimportant.

b. Both CH_3 and CH_3O disappear mainly by radical-radical termination processes.

c. H and OH are not important chain-carriers under the present conditions.

d. The $(CH_3)_2N$ radical is relatively stable at these low temperatures. Its reaction with NO_2 produces CH_3NO, which in turn produces NO for DMNSA formation via reaction (3).

The alternative mechanism for the reaction of $(CH_3)_2N$ with NO_2 directly producing NO:

$$(CH_3)_2N + NO_2 \longrightarrow (CH_3)_2NO + NO \qquad (2b)$$

could not account for the observed DMNSA and CH_3NO_2 profiles, if the stability of the $(CH_3)_2NO\cdot$ radical is assumed to be similar to that of $(CH_3)_2CHO\cdot$, the isopropoxyl radical[17]. The above direct abstraction process was, however, found to be essential for the interpretation of early NO yields in the shock-heated DMNA decomposition reactions[9].

ACKNOWLEDGMENT

Thanks are due to Ms. Jody Beecher for her assistance in analyzing the pyrolysis products.

TABLE I

Reactions and Rate Constants Used in Modeling the Low-Temperature Pyrolysis of DMNA[a]

	Reaction	A	B	E_a	Ref.
(1)	$(CH_3)_2NNO_2 \longrightarrow (CH_3)_2N + NO_2$	3.2 E16	0	45.5	(b)
(2a)	$(CH_3)_2N + NO_2 \longrightarrow 2CH_3NO$	3.0 E12	0	0	(b)
(3)	$(CH_3)_2N + NO \longrightarrow (CH_3)_2NNO$	2.1 E11	0	0	(c)
(4)	$CH_3NO \longrightarrow CH_3 + NO$	5.3 E16	0	42.2	(d)
(5)	$CH_3 + NO_2 \longrightarrow CH_3NO_2$	2.2 E12	0	0	(b)
(6)	$CH_3 + NO_2 \longrightarrow CH_3O + NO$	8.4 E10	.655	-1.00	(d)
(7)	$CH_3 + NO \longrightarrow CH_3NO$	2.4 E12	0	0	(d)
(8)	$CH_3 + (CH_3)_2NNO_2 \longrightarrow CH_4 + NO_2 + CH_2{=}NCH_3$	5.5 E-1	4.0	8.30	(e)
(9)	$2(CH_3)_2N \longrightarrow (CH_3)_2NN(CH_3)_2$	5.6 E11	0	0	(f)
(10)	$CH_3 + (CH_3)_2N \longrightarrow (CH_3)_3N$	1.0 E13	0	0	(g)

TABLE I

Reactions and Rate Constants Used in Modeling the Low-Temperature Pyrolysis of DMNA[a]

(continued)

Reaction	A	B	E_a	Ref.
(11) $CH_3O + NO_2 \longrightarrow CH_2O + HONO$	2.5 E11	0	0	(h)
(12) $CH_3O + (CH_3)_2NNO_2 \longrightarrow CH_3OH + CH_2{=}NCH_3 + NO_2$	2.4 E11	0	7.10	(e)
(13) $CH_3O + NO \longrightarrow CH_2O + HNO$	9.4 E11	0	0	(h)
(14) $CH_3 + (CH_3)_2NNO \longrightarrow CH_4 + NO + CH_2{=}NCH_3$	5.5 E-1	4.0	8.30	(e)
(15) $HCO + NO_2 \longrightarrow HONO + CO$	1.0 E12	0	0	(g)
(16) $HCO + NO \longrightarrow HNO + CO$	7.2 E13	-.40	0	(i)
(17) $CH_2O + CH_3 \longrightarrow HCO + CH_4$	1.0 E11	0	6.10	(j)
(18) $CH_3 + CH_3NO_2 \longrightarrow CH_4 + CH_2NO_2$	2.4 E11	0	9.00	(j)
(19) $CH_2NO_2 + NO_2 \longrightarrow CH_2O + NO + NO_2$	1.0 E11	0	0	(g)
(20) $2CH_3 \longrightarrow C_2H_6$	1.0 E15	-0.64	0	(k)

TABLE I

Reactions and Rate Constants Used in Modeling the Low-Temperature Pyrolysis of DMNA[a]

(continued)

Reaction	A	B	E_a	Ref.
(21) $CH_3 + HNO \longrightarrow CH_4 + NO$	1.0 E11	0	0	(g)
(22) $CH_2NO + NO_2 \rightarrow CH_2O + 2NO$	1.0 E12	0	0	(g)
(23) $CHO + HNO \longrightarrow CH_2O + NO$	3.2 E11	0.5	0	(h)
(24) $(CH_3)_2N + HNO \longrightarrow (CH_3)_2NH + NO$	1.0 E11	0	0	(g)
(25) $2HNO \longrightarrow H_2O + N_2O$	1.0 E9	0	0	(g)
(26) $CH_3O + HONO \longrightarrow CH_3OH + NO$	1.0 E12	0	0	(g)
(27) $HNO + HONO \longrightarrow H_2O + 2NO$	1.0 E9	0	0	(g)
(28) $2HONO \longrightarrow H_2O + NO + NO_2$	1.0 E9	0	0	(g)
(29) $2CH_3O \longrightarrow CH_2O + CH_3OH$	1.1 E13	0	0	(k)
(30) $CH_3 + CH_3O \longrightarrow CH_4 + CH_2O$	2.4 E13	0	0	(k)
(31) $CH_3 + CH_3O \longrightarrow CH_3OCH_3$	1.2 E13	0	0	(k)

TABLE I

Reactions and Rate Constants Used in Modeling the Low-Temperature Pyrolysis of DMNA[a]

(continued)

Reaction	A	B	E_a	Ref.
(32) $CH_3O + CH_2O \longrightarrow CH_3OH + CHO$	1.0 E11	0	0	(k)
(33) $(CH_3)_2N + NO_2 \longrightarrow (CH_3)_2NNO_2$	6.0 E11	0	0	(d)
(34) $(CH_3)_2NN(CH_3)_2 \longrightarrow 2(CH_3)_2N$	2.5 E8	0	0	(f)

(a) Rate constants, in the form: $k = AT^B \exp(-E_a/RT)$, are in cc $mole^{-1}$ sec^{-1} and E_a, kcal mol^{-1}.
(b) This study.
(c) Computer fitted from DMNSA + NO_2 and DMNA shock tube expts[7,9].
(d) RRKM calculations
(e) Estimated from the analogous C_2H_6 reaction. C_2H_6 data from (k).
(f) RRKM calculations, from data of D.M. Golden, R.K. Solly, N.A. Gac and S.W. Benson, Int. J. Chem. Kinet., 4, 433 (1972), temperature dependent, value listed for 472K.
(g) Assumed.
(h) F. Westley, "Table of Recommended Rate Constants for Chemical Reactions Occurring in Combustion", NSRDS-NBS, 67, National Bureau of Standards, Washington, D.C. (1980).
(i) B. Veyret and R. Lesclaux, J. Phys. Chem. 85, 1918 (1981).
(j) J.A. Kerr and M.J. Parsonage, "Evaluated Kinetic Data on Gas Phase Hydrogen Transfer Reactions of Methyl Radicals", Butterworth, London, 1976.
(k) W. Tsang, Combustion Kinetic Data Survey, NBS, to be published.

Table II

Rate Constants (k_5) for $CH_3 + NO_2 \longrightarrow CH_3NO_2$

T/K	$k_5/10^{12}$ cc·mole^{-1}sec^{-1}
472.3	2.6
474.1	2.1
478.2	2.2
483.5	1.5
490.2	1.7
495.2	2.1
504.1	2.9
507.6	2.1
513.8	2.5
524.3	2.7
363.2	1-12[a]

a. L. Phillips and R. Shaw (10th Symp. (International) on Combustion, p. 453, 1965) measured the ratio of k_5/k_7 to be 1.7 at 363.2 K. According to CRC Handbook of Bimolecular and Termolecular Reactions (J.A. Kerr and S.J. Moss) Vol. II, P. 38, CRC Press, 1981, the values of k_7 vary from 5×10^{11} to 6×10^{12}cc/mole sec. Specifically, the value obtained by Basco et al. (Ref. 15), $2.4 \pm 0.2 \times 10^{12}$ cc/mole sec., on which k_4 was based in our kinetic modeling, gives rise to $k_5 = 4.2\times10^{12}$ cc/mole sec. This is in close agreement with our average value, $k_5 = 2.2 \pm 0.5 \times 10^{12}$ cc/mole sec.

References

1. J. M. Flournoy, J. Chem. Phys., 36, 1106 (1962).

2. B. L. Korsunskii and F. I. Dubovitskii, Dokl. Akad. Nauk. SSSR 155, 402 (1964).

3. B. L. Korsunskii, F. I. Dubovitskii, and G. V. Sitonina, Dokl. Akad. Nauk SSSR 174, 1126 (1967).

4. D. F. Golden, J. R. Barker, K. E. Lewis, P. L. Trevor, and D. M. Golden, UCRL-15104, Jan. 31, 1980, NTIS, Springfield, Va.

5. W. J. Chute, K. G. Herring, L. E. Toombs, and G. W. Wright, Can. J. Research (B) 26, 89 (1948).

6. M. E. Umstead, J. Chromatog. Sci. 12, 106 (1974).

7. M. E. Umstead, S. A. Lloyd, D. S. Y. Hsu, and M. C. Lin, "Proceedings of the 21st. JANNAF Combustion Meeting", Laurel, Md., 1984, p. 417, CPIA, Laurel, Md.

8. M. E. Umstead, S. A. Lloyd, and M. C. Lin, "Proceedings of the 22nd. JANNAF Combustion Meeting", Pasadena, CA, 1985. In press. CPIA, Laurel, MD.

9. M. E. Umstead and M. C. Lin, to be published.

10. R. Shaw and F. E. Walker, J. Phys. Chem., 81, 2572 (1977).

11. Y. T. Lee, private comm.

12. J. D. Cox and G. Pilcher, "Thermochemistry of Organic and Organometallic Compounds", Academic Press, 1970.

13. D. F. McMillen and D. M. Golden, Ann. Rev. Phys. Chem., 33, 493 (1982).

14. L. Batt, B. G. Gowenlock, and J. Trotman, J. Chem. Soc., 2222 (1960).

15. N. Basco, D. G. L. James, and R. D. Suart, Int. J. Chem. Kinet., 2, 215 (1970).

16. B. G. Gowenlock and D. R. Snelling, in ACS Adv. in Chem. Series, 36, "Free Radicals in Inorganic Chemistry", p. 150, 1962.

17. L. Batt, Int. J. Chem. Kinet., 11, 977 (1979).

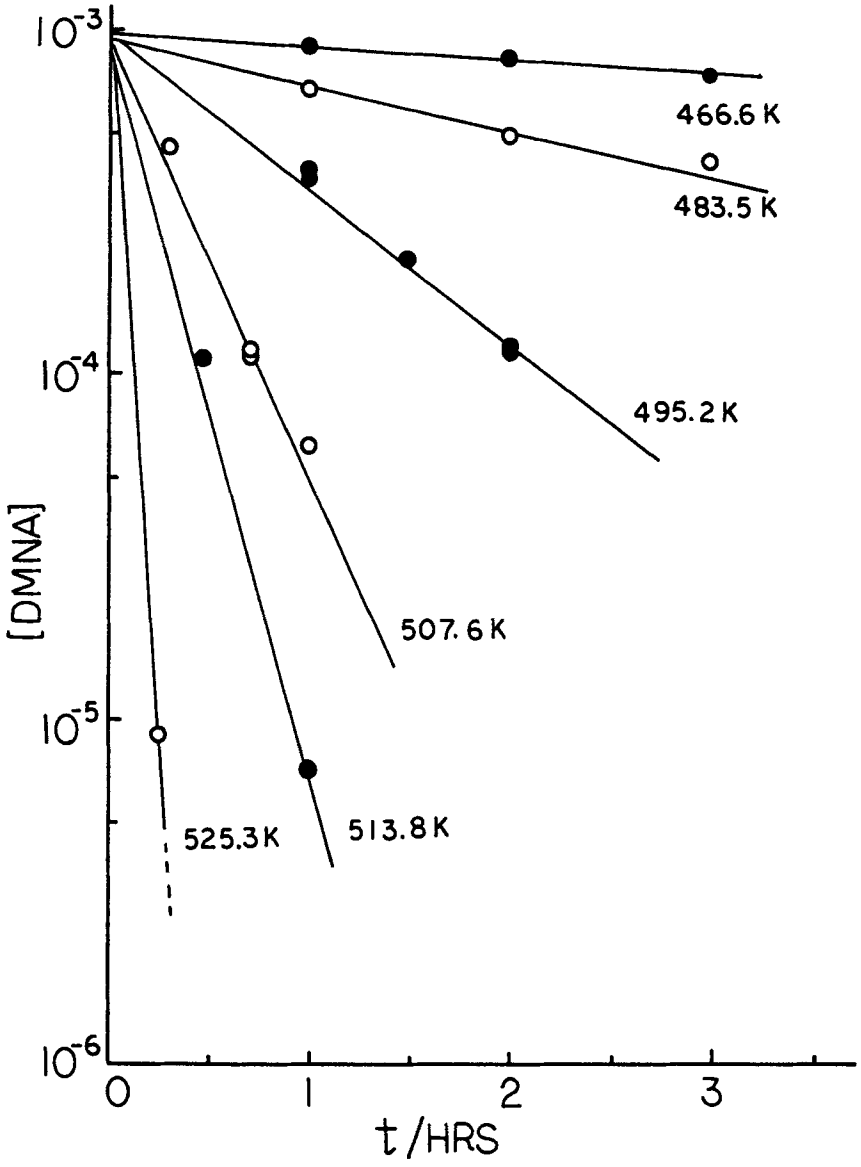

FIGURE 1

DMNA disappearance as functions of temperature and time. 475 torr pure DMNA.

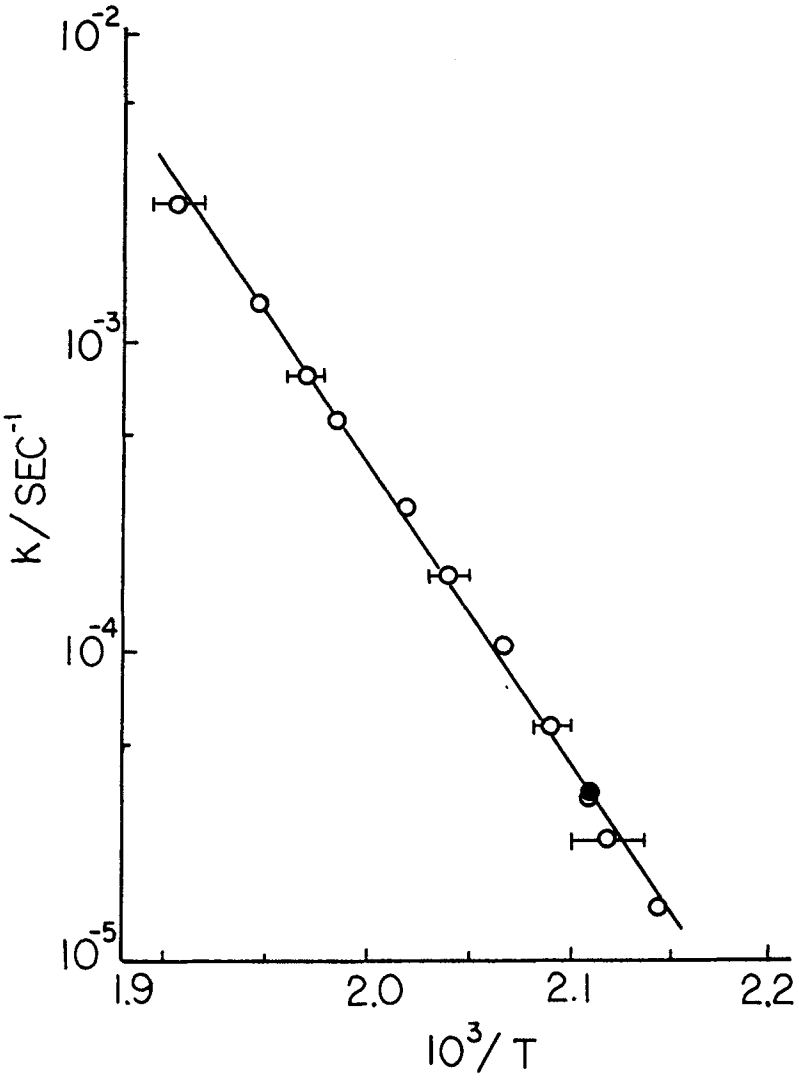

FIGURE 2

Arrhenius plot of the rate constants for DMNA thermal decomposition from 466 to 524 K. 475 torr pure DMNA. Filled circle: 881 torr toluene added.

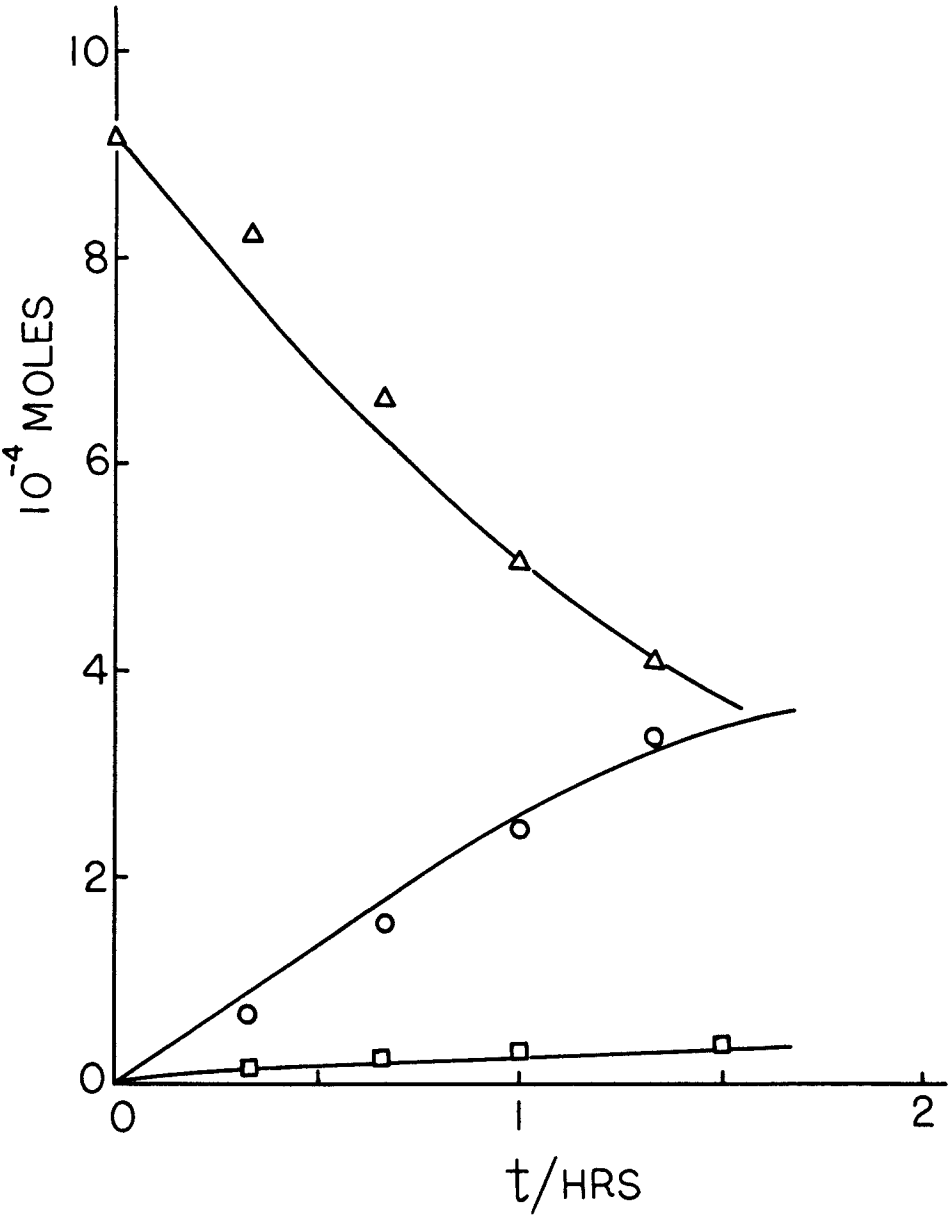

FIGURE 3

Rate of DMNA disappearance and DMNSA and CH_3NO_2 formation in the thermal decomposition of DMNA at 490 K. Triangles: DMNA, circles: DMNSA, squares: CH_3NO_2. Solid lines: computed curves.

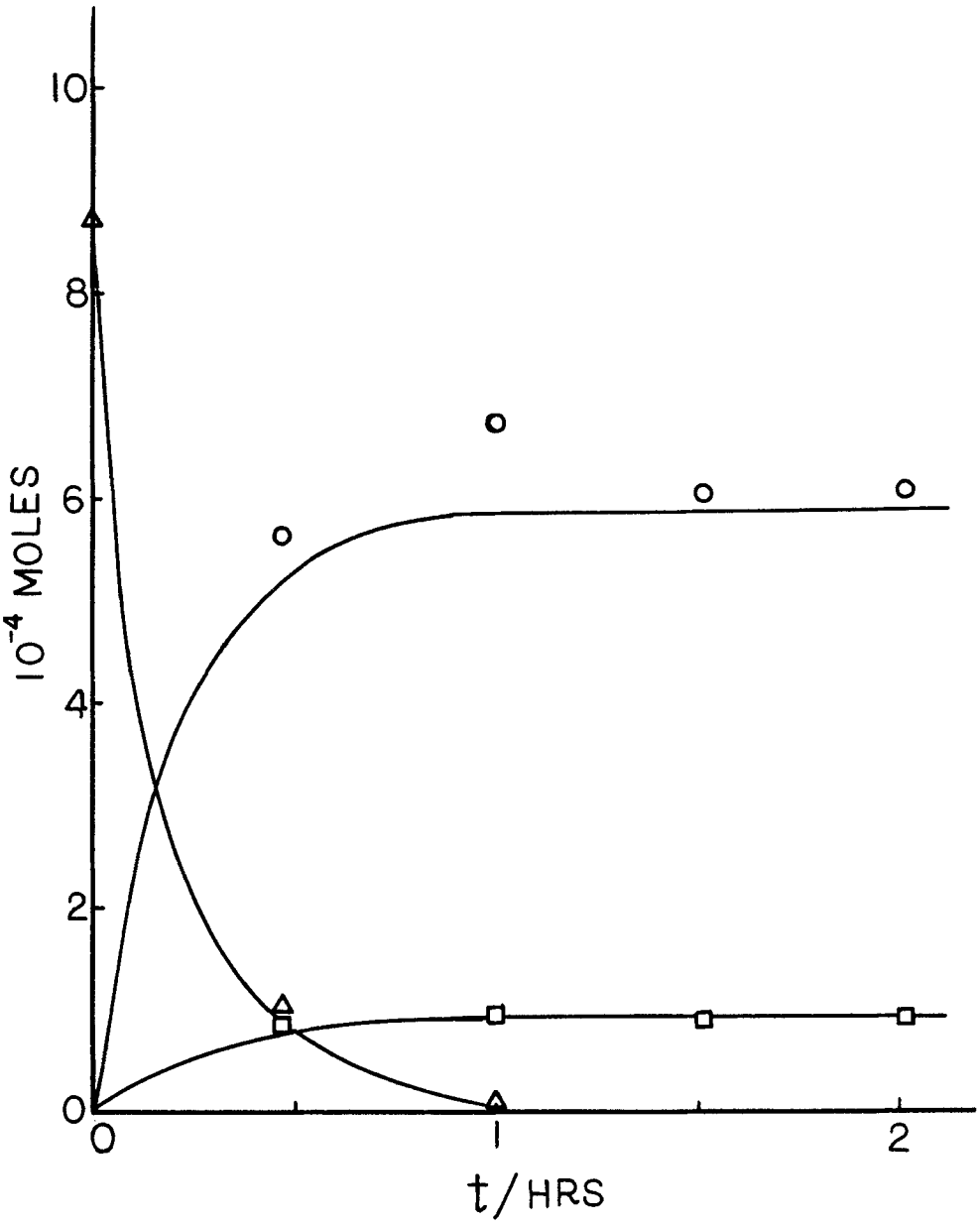

FIGURE 4

Rate of DMNA disappearance and DMNSA and CH_3NO_2 formation in the thermal decomposition of DMNA at 514 K. Triangles: DMNA, circles: DMNSA, squares: CH_3NO_2. Solid lines: computer curves.

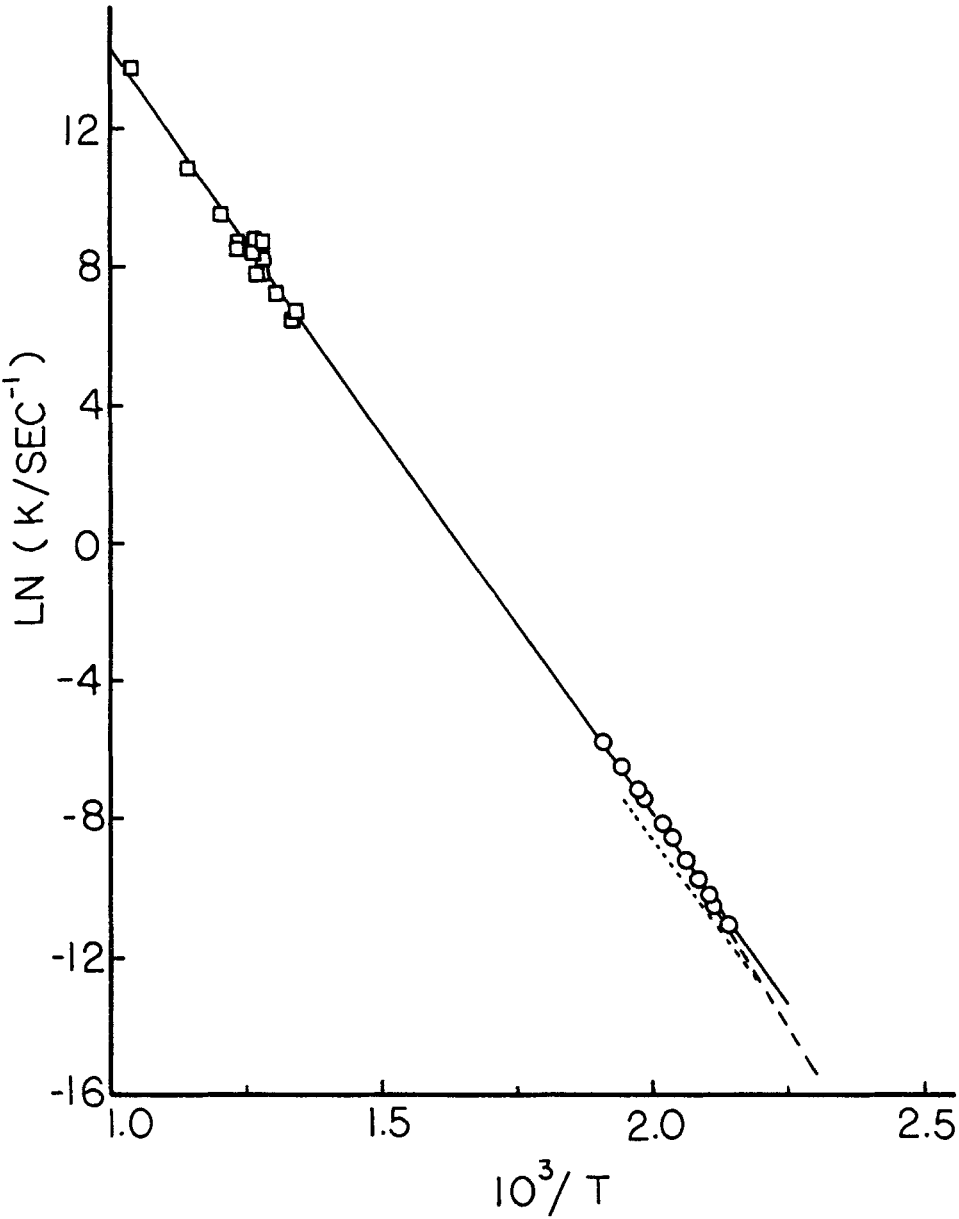

FIGURE 5

Arrhenius plot of the rate constants for DMNA thermal decomposition from 466 to 959 K. Circles: low-temperature pyrolysis results (this work), squares: shock tube results (Ref. 9). Dotted line: Korsunskii and Dubovitskii (Ref. 2), dashed line: Flournoy (Ref. 1).

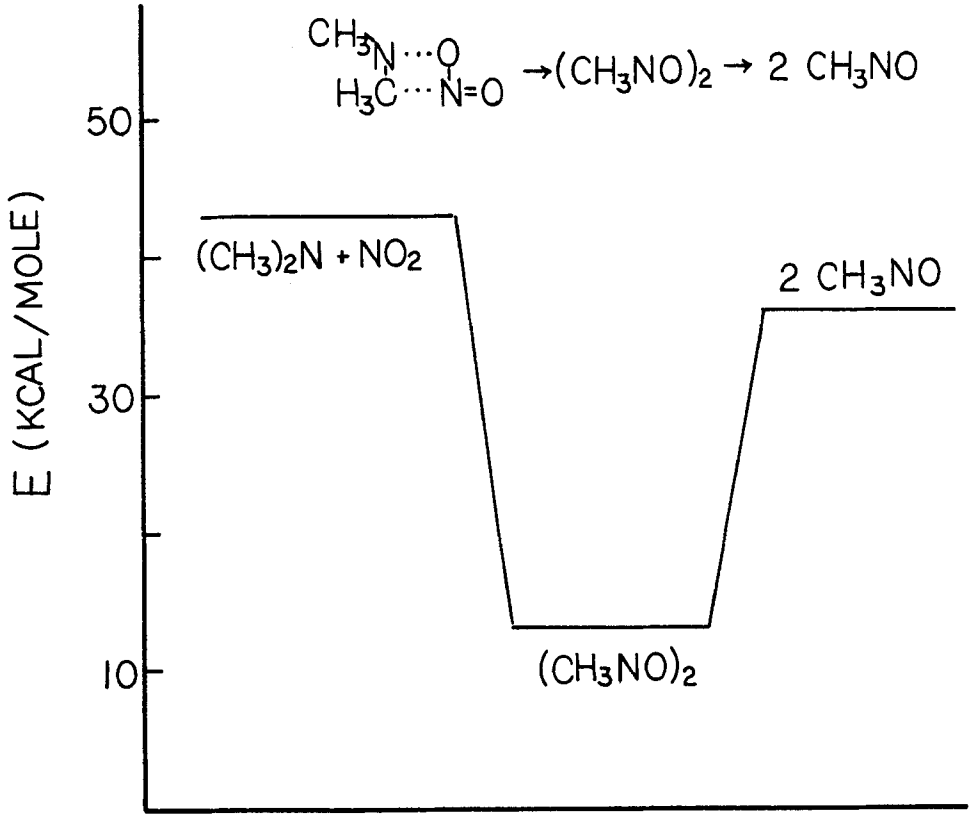

FIGURE 6

Energy diagram for the reaction of NO_2 with the dimethylamino radical.